A Liquid Air Energy Storage System Utilizing Upgraded LNG Cold Energy for Air Liquefaction

Jiamin Du[1,2], Zhikang Wang[1,2], Junxian Li[1,2], Yihong Li[1,2], Xiaoyu Fan[1,2], Zhaozhao Gao[1,4], Wei Ji[3,*], Liubiao Che[1,2,3], Junjie Wang[1,2,4,*]

[1] State Key Laboratory of Cryogenic Science and Technology, Technical Institute of Physics and Chemistry, Chinese Academy of Sciences, Beijing 100190, China;
[2] University of Chinese Academy of Sciences, Beijing 100049, China;
[3] Institute of Optical Physics and Engineering Technology, Qilu Zhongke, Licheng District, Jinan 250100, China.
[4] Zhonglv Zhongke Energy Storage Technology Co., Ltd., 18 Lishi Hutong, Dongcheng District, Beijing, P. R. China

[*]Corresponding author. E-mail: ji-wei@cgdg.com (Dr. Wei Ji)
wangjunjie@mail.ipc.ac.cn (Prof. Junjie Wang)

Abstract. Liquid air energy storage (LAES) offers high energy density and geographical flexibility, making it a promising large-scale storage technology. However, conventional cold storage methods, including liquid-phase and solid-phase storage, suffer from inherent limitations, underscoring the need for more efficient and reliable cold storage solutions to improve LAES performance. This study proposes the integration of cold energy released during liquefied natural gas (LNG) vaporization into the LAES system. By employing a compression refrigeration cycle, the LNG cold energy is upgraded to a temperature range suitable for high-pressure air liquefaction. Nitrogen is utilized as the working fluid in this cycle to eliminate safety risks associated with the direct interaction of LNG and air within the same heat exchanger. This approach lowers costs, enhances safety, and improves cold storage performance. Moreover, the cold energy from liquid air is recovered through Organic Rankine Cycles to generate electricity, further improving the system's overall energy utilization. A thermodynamic model of the proposed system is developed, and the impacts of critical parameters, including compression pressure, liquefaction rate, and expansion pressure, on the round-trip efficiency of the LAES system are thoroughly analyzed. The results provide valuable insights for optimizing cold storage in LAES systems.

1. Introduction

In recent years, the increasing frequency of extreme weather events and the rise in global temperatures have drawn significant international attention, prompting a global shift toward cleaner energy sources. According to projections by the International Energy Agency, renewable energy is expected to account for more than 42% of global electricity generation by 2028 [1]. However, the intermittent and fluctuating nature of renewable energy presents major challenges to grid integration. These challenges have accelerated the development of energy storage technologies, which, due to their controllability, have emerged as a key solution to the instability of renewable power generation.

Liquid air energy storage (LAES) technology has emerged as a promising large-scale energy storage solution due to its independence from geographical constraints, high energy density, and cost-effectiveness [2]. Since the concept was first proposed in 1977, extensive research has been conducted on LAES systems, with particular focus on improving overall system efficiency and optimizing cold energy storage units [3].

In LAES systems, the recovery and utilization of cold energy constitute one of the most critical and distinctive subsystems. Currently, the most common cold storage methods include liquid-phase and solid-phase cold storage. Solid-phase storage beds typically use inert materials such as stones, quartzite, and granite pebbles as the thermal storage medium, offering advantages such as low cost and environmental friendliness [4]. However, their thermal efficiency is generally lower than that of liquid-phase storage, which remains a major barrier to large-scale adoption. Guo et al. [5] investigated the coupling between solid-phase thermal storage beds and LAES systems, analyzing both multi-cycle performance and dynamic responses under different operational modes. Considering intermittent operation and cold energy loss, the quasi-steady-state cycle efficiency of the LAES system was found to be 16.8% lower than that of the ideal cycle.

Liquid-phase cold storage media, such as propane and methanol-water solutions, offer higher efficiency compared to solid-phase counterparts [6]. However, the flammability and explosive potential of these substances pose significant safety concerns.

In recent years, liquefied natural gas (LNG) has played an increasingly prominent role as a transitional energy source. Peng et al. [7] proposed a coupled LAES-LNG-CS system in which the cold energy released during the LNG regasification process is recovered using propane, compressed, and stored to assist in the liquefaction of high-pressure air. She et al. [8] integrated the surplus heat generated in the LAES system with the cold energy from LNG regasification through a Brayton cycle. In this configuration, the waste heat from the LAES system serves as the heat source, while the cold energy from LNG regasification acts as the cold source, thereby enhancing the overall power output of the system.

Building upon these studies, this paper proposes the use of a compression refrigeration cycle to upgrade the quality of cold energy from LNG regasification, replacing the cold energy storage unit in the LAES system.

2. System description

Figure 1 illustrates the schematic flow diagram of the system. In the energy storage phase, air passes through a multi-stage compression unit (A1-A7), where it is compressed and intercoolers are used to store the generated heat in hot water. The high-pressure air is then directed to the liquefaction unit for further processing.

In the secondary liquefaction stage, LNG (L1) is pumped and pressurized. The pressurized LNG (L3) enters the intercooler (IC4), where it precools nitrogen gas (N3) exiting the liquefaction heat exchanger (LHE3), resulting in N4. This process reduces the power consumption of the compressor (COM). Subsequently, L1 is routed into LHE4 to further cool the compressed nitrogen (N5). The cooled nitrogen (N1) is then expanded in the expander (TUR) to a lower temperature (N2) and enters LHE3 to liquefy the high-pressure air, thereby completing the cycle.

The LNG (L4), after heat exchange in IC4 and LHE4, enters the primary liquefaction stage through LHE2, providing cooling capacity to nitrogen (N6-N9) and participating in the air liquefaction process in LHE1. The low-grade residual cold energy of LNG, after providing cooling for the primary unit, is further utilized before being delivered to the end user.

In the energy release phase, the liquefied air is pressurized via a cryogenic pump and introduced into the ORC unit, where the cold energy released during vaporization (A14-A18) is recovered. The air is then sent to the expansion unit, where it is reheated by the pre-expander heater and expanded in the expander (A18-A24) to perform work.

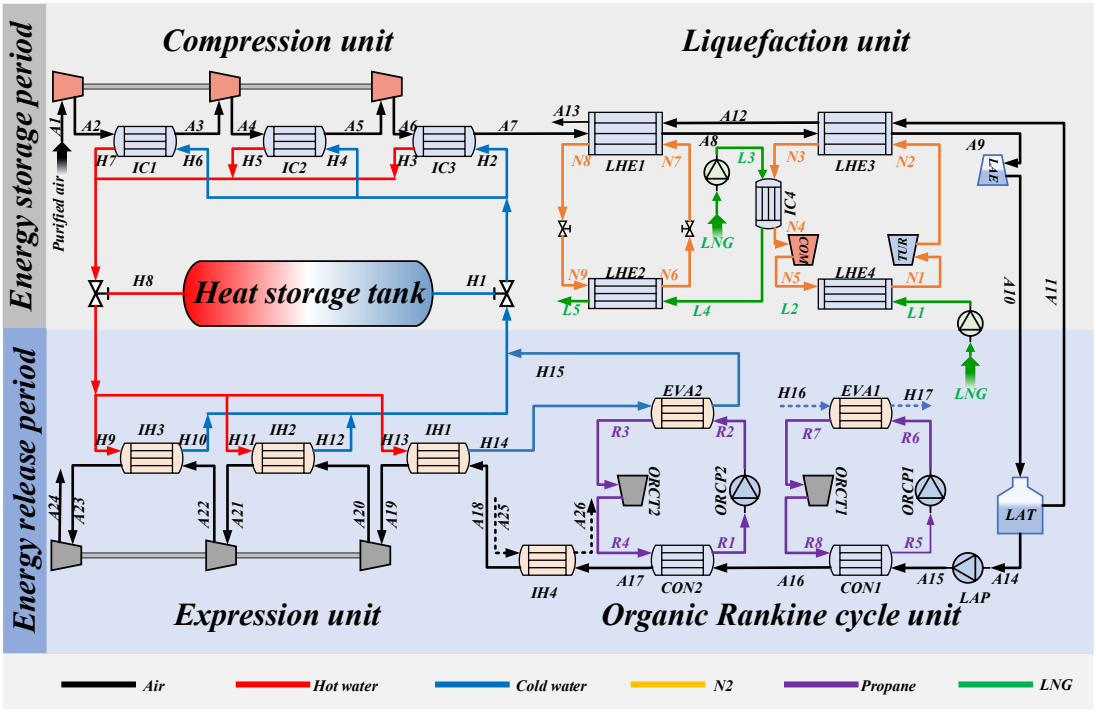

Figure 1. Conceptual design of the system.

3. Method

The computational work in this study was carried out using the Aspen HYSYS software platform. Aspen HYSYS is a powerful process simulation and optimization tool with both steady-state and dynamic simulation capabilities, enabling the design, optimization, and performance analysis of complex industrial processes. In this research, a system process model was constructed within the software to simulate the energy exchange among various components, including the input power of compressors, the output power of expanders, and the heat transfer rates of heat exchangers. The analyses presented in Section 4 were based on the performance data provided by Aspen HYSYS, combined with the thermodynamic equations described in Section 3, to ensure the accuracy and reproducibility of the results.

This study focuses on comparing the system performance under different parameter settings rather than reproducing all physical details at the component design level. Therefore, to improve computational efficiency while ensuring accuracy in system-level thermodynamic evaluation, the model was appropriately simplified. The simplified process is illustrated in Figure 1. In addition, to avoid the computational complexity caused by variations in humidity or trace components of

air, the working fluid was assumed to be dry and pure with a fixed composition. The specific proportions and other assumptions adopted in this study are as follows:

1) The air is pure and dry, air consisting of nitrogen (78.12%), oxygen (20.96%), and argon (0.92%).
2) The operating conditions of all units are stable.
3) All fluid parameters in the simulation are based on the Peng-Robinson equation.
4) In this paper, the liquefaction unit employs the plate-fin heat exchanger with a pinch temperature of 2 K, while other heat exchangers adopt shell-and-tube heat exchangers with a pinch temperature of 10 K.
5) The composition of LNG is shown in Table 1.
6) The basic parameters of this system are shown in Table 2.

Table 1. The composition of LNG.

LNG	Molar ratio
Nitrogen	0.0012
Methane	0.9115
Ethane	0.0555
Propane	0.0216
n-Butane	0.0051
i-Butane	0.0051

Table 2. The basic parameters of this system.

Items	Values
LNG inlet pressure	1.1 bar
Air compression pressure	70.2 bar
Air expansion pressure	160.0 bar
Charging time	8 h
Discharging time	8 h
Compressor isentropic efficiency	85%
Turbine isentropic efficiency	85%

In this study, system performance is evaluated and calculated based on the thermodynamic models of each component.

For the ORC unit, the efficiency can be defined as the ratio of the net output power of the ORC to the input of energy.

$$\eta_{ORC} = \frac{W_{ORCT} - W_{ORCP}}{m \times (h_{in} - h_{out})} \quad (1)$$

where, W_{ORCT} is the power output of the ORCT, W_{ORCP} is the power consumed by the ORCP, m is the mass flow rate of the working fluid in the ORC, kg/s； h_{in} and h_{out} are the enthalpy of the fluid supplying the heat source to the ORC system at the inlet and outlet, respectively, kJ/kg.

RTE is defined as the ratio of the net output power during peak periods of the system to the net input power during valley periods of the system.

$$RTE = \frac{W_{ATs} - W_{LAP} + W_{ORCT1} + W_{ORCT2}}{W_{ACs} - W_{LAE} + W_{COM} - W_{TUR} + W_{ORCP1} + W_{ORCP2}} \quad (2)$$

where, W_{ATs} is the power output of the air turbines, kW, W_{LAP} is the power input of the LAP, W_{ACs} is the power consumption of the compressors, W_{LAE} is the power output of the LAE, kW, W_{COM} is the net power consumption of the COM, kW, W_{TUR} is the net power output of the TUR, kW, W_{ORCT1}, W_{ORCT2} are the net power output of the ORCT1, ORCT2, kW, W_{ORCP1}, W_{ORCP2} are the net power input of the ORCP1, ORCP2, kW.

4. Result discussion

This study analyzed the system's performance by investigating the effects of key parameters, such as the number of compression stages and expansion pressure, to provide a clearer understanding of the system performance. Although the overall system structure shown in Figure 1 remains unchanged, variations in the number of compression stages affect the intercooling process in the compression unit (A1–A7), thereby influencing compression power consumption. Similarly, changing the expansion pressure modifies the operation of the expansion unit (A18–A26), altering the output work. These two parameters were chosen because they directly govern the input and output terms of RTE, making them the most influential factors for evaluating overall system performance.

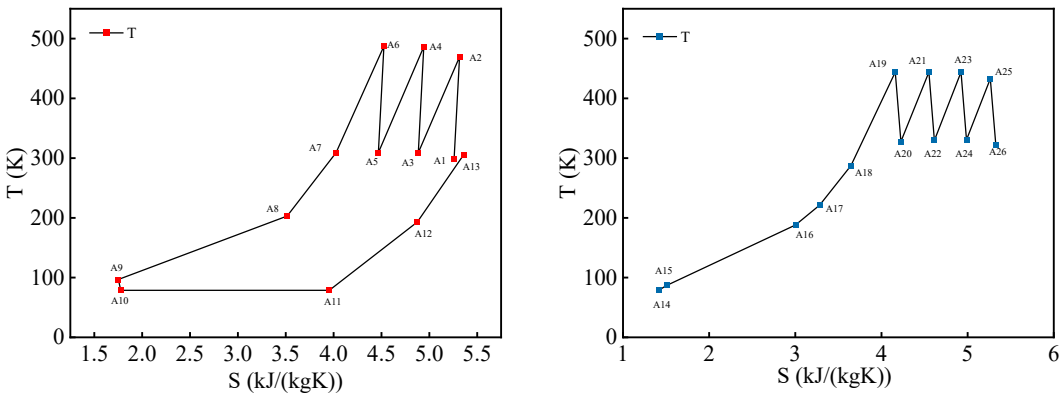

Figure 2. Temperature-entropy diagrams (air compression process and air expansion process).

Figure 2 depicts the temperature–entropy (T–s) diagrams of the air compression and expansion processes in the proposed LAES–LNG system. The left-hand diagram corresponds to multi-stage compression during the charging phase (A1–A10), while the right-hand diagram shows the reheating and expansion process during the discharging phase (A14–A26). These diagrams provide thermodynamic insight into how variations in compression stages and

expansion pressure influence system performance. Table 3 shows parameters such as temperature and pressure at critical nodes of the system.

Table 3. System critical node parameters.

Fluids	Temperature	Pressure
H1	298.15 K	4.00 bar
H8	455.05 K	4.00 bar
A1	298.15 K	1.00 bar
A7	309.15 K	70.19 bar
A8	203.15 K	70.14 bar
A9	96.95 K	70.09 bar
A10	78.95 K	1.00 bar
A14	78.95 K	1.00 bar
A15	87.35 K	160.00 bar
A18	287.15 K	160.00 bar
A24	322.75 K	1.00 bar

4.1 Effect of the number of compression stages on the proposed system

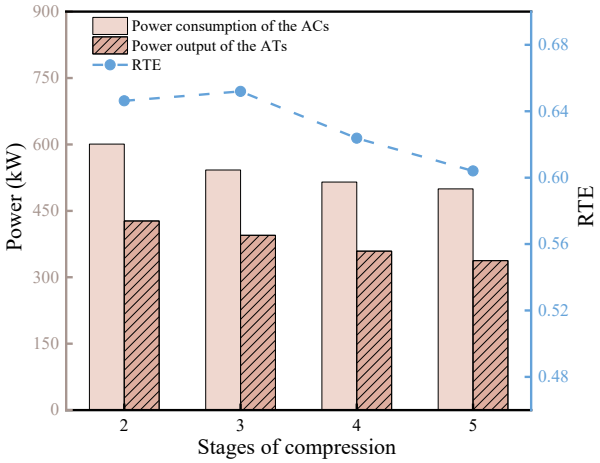

Figure 3. The RTE of the system under different compression stages.

Figure 3 illustrates the relationship between the number of compression stages and the system's round-trip efficiency (RTE), while also comparing the compression power consumption and expansion work under different compression stages.

As the number of stages increases from two to four, the system RTE first increases and then decreases, reaching a maximum at three stages. The figure shows that increasing the number of stages leads to a gradual reduction in compression power consumption. This is because more stages make the compression process closer to isothermal compression, thereby reducing the energy required. However, the expansion work decreases with more stages due to the lower temperature of compression heat, which reduces the heating temperature during the discharge phase and subsequently lowers the expansion output. The three-stage configuration strikes an optimal balance—achieving relatively low compression energy consumption while maintaining sufficient expansion work—thus resulting in the highest system RTE.

4.2 Effect of the expansion pressure on the proposed system

Figure 4 illustrates the relationship between the system's RTE and the expansion pressure.

As the expansion pressure increases from 135 bar to 160 bar, the RTE improves from 63.6% to 65.1%, and the output power of the expansion unit rises from 384 kW to 394 kW. This improvement is attributed to the enhanced work capacity of the air at higher expansion pressures. In practical engineering applications, the expansion pressure should be maximized within the allowable limits of heat exchangers and other system components to optimize system performance.

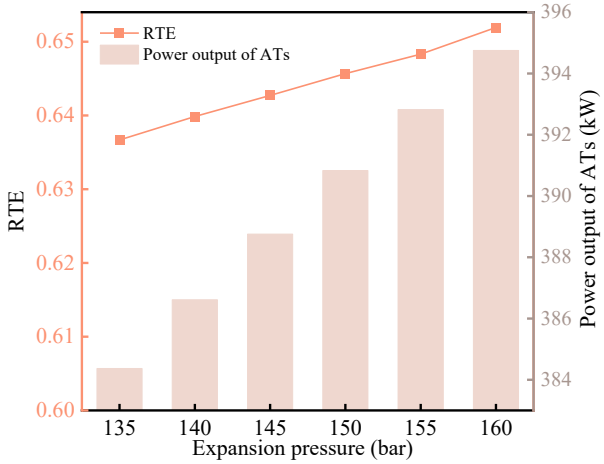

Figure 4. The RTE of the system under different expansion pressure.

4.3 The influence of the different ORC working fluids on system

In this study, two ORCs are employed to recover the cold energy released during the discharge phase of liquid air. The working fluids for the ORCs are selected from organic substances suitable for low-temperature waste heat recovery. A preliminary comparison was conducted among several candidates, including propane, R143a, R125, R600a, and R32. As shown in Figure 5, when propane is used as the working fluid, both ORC units achieve the highest efficiency, contributing the most to the system's overall power output and resulting in the highest RTE.

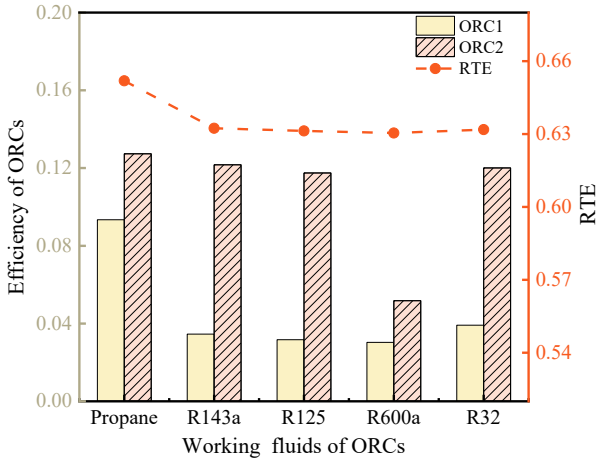

Figure 5. The influence of the different ORC working fluids on system.

5. conclusion

The coupling between LAES and LNG not only enhances energy utilization efficiency but also offers a novel approach for innovating and optimizing cold energy storage systems. This study employs a compression refrigeration cycle to upgrade the cold energy released during the regasification of LNG, thereby replacing the cold storage unit in conventional LAES systems. The system parameters were optimized and designed accordingly. As the number of compression stages increases, the RTE initially rises and then declines, with the optimal configuration determined to be three-stage compression. The influence of expansion pressure on system performance was also investigated. Results indicate that RTE increases with expansion pressure; therefore, the expansion pressure should be appropriately increased within the allowable limits of the equipment to improve system efficiency. In addition, various working fluids for ORCs were evaluated, and propane was identified as the most effective medium under the proposed process.

Acknowledgments

This work is supported by the National Key Research and Development Program of China (2024YFE0208500), the Postdoctoral Fellowship Program of CPSF (GZC20241778), and technological innovation projects of China Green Development Investment Group Co., Ltd. (No. 09CHDD020 and No. 09CHDD021).

References

[1] IEA (2024), *Share of renewable electricity generation by technology, 2000-2028*, IEA, Paris.
[2] Fan X, Li J, Gao Z, Chen L and Wang J 2024 Appl. Energy **355** 122236.
[3] Ameel B, T'joen C, Kerpel D, Jaeger D, Huisseune H, Belleghem V, Paepe D 2013 Appl. Therm. Eng. **52** 130-140.
[4] Li J, Fan X, Li Y, Wang Z, Gao Z, Ji W, Chen L and Wang J 2024 J. Energy Storage **86** 111359.
[5] Guo L, Ji W, Gao Z, Fan X and Wang J 2021 J. Energy Storage **40** 102712.
[6] Fan X, Xu H, Li Y, Li J, Wang Z, Chen L and Wang J 2024 Appl. Energy **371** 123739.
[7] Peng X, She X, Li C, Luo Y, Zhang T, Li Y and Ding Y 2019 Appl. Energy **250** 1190-1201.
[8] She X, Zhang T, Cong L, Peng X, Li C, Li Y and Ding Y 2019 Appl. Energy **251** 113355.